

Can electroweak bubble walls run away?

Dietrich Bödeker

Fakultät für Physik, Universität Bielefeld, D-33501 Bielefeld, Germany

Guy D. Moore

Department of Physics, McGill University,

3600 rue University, Montréal, QC H3A 2T8, Canada and

Fakultät für Physik, Universität Bielefeld, D-33501 Bielefeld, Germany

(Dated: March 2009)

Abstract

In extensions of the Standard Model with SU(2) singlet scalar fields, there can be regions of parameter space for which the electroweak phase transition is first order already at the mean-field level of analysis. We show that in this case the phase interface (bubble wall) can become ultra-relativistic, with the relativistic gamma factor $\gamma = (1 - v_{\text{wall}}^2)^{-1/2}$ growing linearly with the wall's propagation distance. We provide a simple criterion for determining whether the bubble wall “runs away” in this way or if γ approaches a terminal value.

I. INTRODUCTION

Electroweak symmetry breaking is a central feature of the Standard Model, arising because the Lagrangian mass squared for the Higgs field is negative. However, interaction with a thermal medium rather generically raises the effective (thermal) mass squared of scalar particles, leading to high temperature symmetry restoration [1, 2]. Such symmetry restoration is expected in the Standard Model at temperatures of order $T \sim m_H \sim 100\text{GeV}$, which presumably occurred very early in the hot Big Bang.

Such symmetry breaking in a gauge-singlet scalar field would automatically imply a thermal phase transition between symmetry-restored (high temperature) and symmetry broken (low temperature) phases.¹ But the Higgs field (or fields) transforms nontrivially under a nonabelian gauge symmetry. The notions of vacuum expectation value and symmetry breaking for such a scalar are only defined perturbatively, and there is no guarantee that there will be a phase transition associated with electroweak symmetry breaking [4]. In particular, within the Minimal Standard Model at allowed values for the Higgs mass, no electroweak phase transition exists [5]. But an electroweak phase transition would occur in numerous phenomenologically interesting extensions of the Standard Model. Such a transition is interesting cosmologically for a number of reasons:

- A first order electroweak phase transition might lead to electroweak baryogenesis [6, 7], giving rise to the baryon number observed in the universe today.
- A first order phase transition might produce primordial magnetic fields [8, 9] which might seed the formation of today's galactic and extragalactic magnetic fields.
- A first order electroweak phase transition might give rise to observable gravitational wave backgrounds [10, 11, 12] in interesting frequency ranges for future experiments (around 10^{-3} Hertz).

There are two key attributes of the transition which are important in these scenarios. One is the strength of the electroweak phase transition (for instance, the available free energy and latent heat as a fraction of the energy density of the electroweak plasma). This is determined by model parameters (field content, masses and coupling constants) which are not known. However we have developed the theoretical tools for determining the strength of the transition, given the model parameters [13]. The other attribute is the bubble wall velocity, meaning the propagation speed of the interface between high temperature and low temperature phases, while the transition is taking place. This velocity is relevant to all physical consequences of the phase transition. In particular:

- Electroweak baryogenesis scenarios seem to be quite sensitive to the bubble wall velocity [14, 15, 16, 17, 18]. A slow bubble wall allows nonequilibrium conditions to exist “in front” of the bubble wall, in the symmetric electroweak phase where baryon number violating processes are fast [14]. A thin, very fast bubble wall would provide a

¹ It is possible in some models to have thermal effects induce symmetry breaking, rather than restoration [3]. But this requires rather special coupling relations and is not important to the rest of our discussion.

nonequilibrium environment only in the broken phase, probably making baryogenesis very inefficient.

- Gravitational waves are of maximum strength if the bubble walls are highly relativistic. Slow subsonic bubble walls give rise to rather extended and smooth hydrodynamic waves, which should be poor sources of gravitational waves (see [19] for the hydrodynamics of transitions with finite bubble wall velocities). On the other hand, if the bubble walls propagate ultra-relativistically and a nontrivial fraction of the free energy density of the plasma goes into their acceleration, it could give rise to very interesting gravitational wave signals.²

In a first-order cosmological phase transition in vacuum [22], the energy density of the false vacuum is completely converted into kinetic energy of the bubble walls. As a result, the wall velocity keeps increasing and approaches the speed of light ($\gamma \equiv 1/\sqrt{1-v^2}$ grows linearly with the distance a bubble wall propagates). Either this behavior, or highly relativistic walls but with a terminal γ factor, have often been assumed in the gravitational wave literature [11]. On the contrary, the electroweak baryogenesis literature has generally assumed that interactions with the plasma impede the bubble wall and keep its velocity subsonic, $v < 1/\sqrt{3}$, as the rather limited literature computing the wall velocity suggests $v < 0.2$ [23, 24, 25, 26, 27, 28, 29].

The goal of this paper is to determine under what situations the electroweak bubble wall can “run away” and propagate with macroscopic gamma factor $\gamma \equiv (1-v^2)^{-1/2} \gg 1$, and when it more modestly propagates with $\gamma v \lesssim 1$. At the thermodynamic level, we show in Appendix A that runaway walls are logically possible under quite weak conditions; but whether they actually occur depends on how much entropy is produced by the passing wall, which is a problem in the microscopic wall dynamics. However, the relevant physics is actually quite simple, and the right tools already exist in the literature. This paper could have been written more than 10 years ago. However we find that the results neither appear in the literature nor are well known by either community.

Generally, at the mean field level models without electroweak SU(2) singlet scalar fields predict a second order electroweak phase transition. The transition in such a theory *may* be a so-called “fluctuation induced” first order transition (as for the Standard Model with an unphysically light Higgs field). We will show that the bubble wall never runs away in such transitions. On the other hand, theories with SU(2) singlet scalars can in some cases provide a first-order electroweak (SU(2) breaking) phase transition already at the mean-field level of analysis. This is true for instance in the nMSSM [30] (though not for the MSSM). Indeed,

² Steinhardt has argued [20] that bubble walls cannot approach the speed of light if there is a plasma present. However this result was based on assuming that the Chapman-Jouguet condition is fulfilled, that is, that the plasma behind the wall moves at the speed of sound with respect to the wall. This assumption makes sense for burning detonations, where the (chemical) free energy is released behind rather than at the shock, in a region thick enough to apply hydrodynamics; then the fluid must be subsonic in order to push the shock. But, as carefully demonstrated by Laine [21], this assumption is not valid for cosmological phase transitions, where the free energy is liberated internally in the wall; as a result more general detonation solutions are possible. We complete Laine’s treatment in the Appendix, where we show that runaway walls are thermodynamically consistent under quite weak conditions.

as we discuss below, it is true already for the simplest extension of the Standard Model, a theory with an additional real singlet scalar. We will show the such “mean-field first order” electroweak transitions generically, but not invariably, have “runaway” bubble walls, with γ growing linearly with wall propagation distance. We present a simple criterion to determine whether or not such “runaway” will occur.

Specifically, the phase structure is determined by an effective potential $V(h)$ which is the sum of a vacuum part $V_{\text{vac}}(h)$ and a thermal contribution $V_T(h)$. The transition occurs when $V(h) = V_{\text{vac}} + V_T$ has two local minima, a shallower “symmetric” s -minimum and a deeper “broken” h -minimum; the exact criterion for how much deeper the h minimum need be is determined by a bubble nucleation calculation [31]. If replacing $V_T(h)$ with its 2-nd order Taylor approximation³ $(h - h_{\text{sym}})^2 V_T''(h_{\text{sym}})/2$ removes the “broken” minimum or raises it above the symmetric one, the bubble wall cannot run away. If, after this replacement, the “broken” minimum remains deeper than the symmetric one, then the bubble wall will run away. The rest of the paper derives and clarifies this result.

The paper is organized as follows. In Section II we review briefly how the 1-loop thermal effective potential arises. Section III gives a simple derivation of the friction on the electroweak bubble wall when it is propagating ultra-relativistically with respect to the plasma. Section IV illustrates our result using a specific model (a toy version of the nMSSM), showing how to determine whether or not runaway occurs as a function of model parameters. Section V presents some conclusions. There is also an appendix, which discusses the thermodynamic criteria under which runaway walls are consistent.

II. THERMAL EFFECTIVE POTENTIAL: A REVIEW

Our arguments will be based on the way that the thermal effective potential arises from the particles making up the thermal bath. Therefore we start by reviewing this physics. Consider for simplicity a theory of two real scalar fields h, s with tree-level effective potential

$$V_{\text{vac}}(h, s) = \frac{m_H^2}{2} h^2 + \frac{m_S^2}{2} s^2 + \frac{\lambda_H}{4} h^4 + \frac{\lambda_S}{4} s^4 + \frac{\lambda}{4} h^2 s^2. \quad (2.1)$$

At zero temperature we determine the vacuum configuration by seeking the global minimum of the potential with respect to h, s . If, for instance, m_H^2 is negative but m_S^2 and λ are positive, the global minimum will be at $h_0 = \sqrt{-m_H^2/\lambda_H}$ and $s_0 = 0$. In this toy model such a nonzero value spontaneously breaks the $\mathbf{Z}_2 \times \mathbf{Z}_2$ symmetry group down to \mathbf{Z}_2 .

At finite temperature we must take into account, besides the energy density arising from $V_{\text{vac}}(h, s)$, also the energy density of thermal excitations of these (and any other) fields. Fortunately one may define a thermal contribution to the potential $V_T(h, s)$ describing the free energy density of the plasma. The total potential $V = V_{\text{vac}} + V_T$ describes the total free energy as a function of h, s , and its minimum describes the most favored classical background. One efficient way to compute the thermal contributions to $V_T(h, s)$ is differentially (the tadpole method [3]); we compute the derivatives $dV_T(h, s)/dh$ and $dV_T(h, s)/ds$, which can

³ When multiple scalar fields change VEVs at the transition, this expression generalizes to the quadratic form $\frac{1}{2} \sum_{ij} s_i s_j d^2 V / ds_i ds_j$, where s_i runs over all scalars which change VEVs.

be integrated to recover the full potential. In particular, to compute the difference between $V_T(h, s)$ and $V_T(h+\delta h, s)$, calculate the change in all particle energies in changing the value of h :

$$\delta V_T = \sum_a \int \frac{d^3 p}{(2\pi)^3} f_B(E_{p,h,a}) \frac{dE_{p,h,a}}{dh} \delta h = \sum_a \int \frac{d^3 p}{(2\pi)^3} \frac{f_B(E_{p,h,a})}{2E_{p,h,a}} \frac{dm_a^2}{dh} \delta h, \quad (2.2)$$

where the sum \sum_a is over all fields (for us, just h, s), $E_{p,h,a} = \sqrt{p^2 + m_a^2(h, s)}$ and $m_a^2(h, s)$ is the h, s dependent mass squared for particle type a . For a scalar field m^2 is the second derivative of $V(h, s)$ with respect to the scalar field value; for instance, in our toy model $m_s^2(h, s) = m_s^2 + 3\lambda_s s^2 + \lambda h^2/2$.

In addition to this energy cost, there is a free energy cost associated with changing the particle occupancies $f_B(E_{p,h,a})$ from the values relevant at field value h to those relevant at field value $h+\delta h$. But this free energy cost is quadratic in δh , since the equilibrium occupancies are a minimum of the free energy.⁴ Therefore, if we treat δh as infinitesimal we may drop this term, and reconstruct the thermal contribution to the effective potential by integrating Eq. (2.2) – *provided* we account for the way that $E_{p,h,a}$ and $f_B(E_{p,h,a})$ vary with h as we integrate.

Often the particle masses $m_a(h, s)$ are small compared to πT . Then we can approximate $f_B(E)/2E$ in the second expression in Eq. (2.2) with $f_B(p)/2p$. In this case we can perform the integral:

$$\frac{dV_T}{dh} = \sum_a \frac{dm_a^2}{dh} \int \frac{d^3 p}{(2\pi)^3} \frac{f_B(E_{p,h,a})}{2E_{p,h,a}} \simeq \sum_a \frac{dm_a^2}{dh} \int \frac{d^3 p}{(2\pi)^3} \frac{f_B(p)}{2p} = \sum_a \frac{dm_a^2}{dh} \frac{T^2}{24} \quad (2.3)$$

which is trivial to integrate:

$$V_T(h) = \frac{T^2}{24} \sum_a m_a^2(h) + V_0(T), \quad (2.4)$$

with $V_0(T)$ an undetermined (and for us irrelevant) integration constant. A slightly less drastic approximation, useful if $m^2(h_1) - m^2(h_2) \ll T^2$ but valid even if m^2 itself is relatively large, is to neglect the h dependence of the particle masses in the expression for E , replacing $E_{p,h,a}$ with $E_{p,h_1,a}$:

$$V_T(h_2) - V_T(h_1) \simeq \sum_a \left(m_a^2(h_2) - m_a^2(h_1) \right) \int \frac{d^3 p}{(2\pi)^3} \frac{f_B(E_{p,h_1,a})}{2E_{p,h_1,a}}. \quad (2.5)$$

This approximation is the same as determining $V_T(h_2)$ by performing a 2'nd order Taylor series expansion of V_T about h_1 – provided that the potential is at most quartic, and particle squared masses quadratic, in the condensate values of scalar fields (true at tree level in renormalizable theories). In what follows we will call this the mean field approximation to the effective potential. In our toy model, if only the h field takes a nonzero background value, the effective mass for the s field is $d^2 V_{\text{vac}}/ds^2 = m_s^2 + \lambda h^2/2$. In this case the s

⁴ This is an example of the usual perturbation theory result that changes to the state first give rise to shifts in the (free) energy at second order in a perturbation.

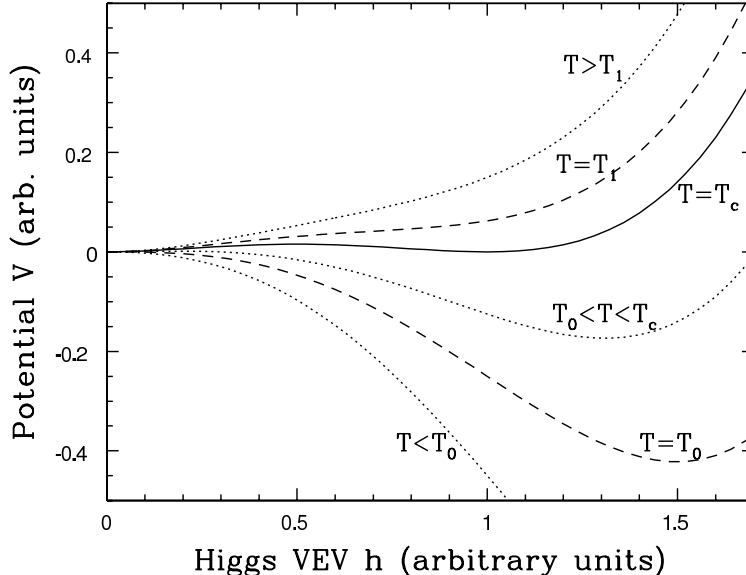


FIG. 1: Example of the potential $V = V_{\text{vac}} + V_T$ in our toy model, for parameters which give a first order transition. The curves are $V(h)$ at a series of temperatures from high (top) to low (bottom); the dotted curves are the potential when the $h = 0$ phase becomes spinodally unstable (T_0) and where the $h \neq 0$ phase becomes unstable (T_1). The solid curve is the potential at the equilibrium temperature (T_c) where both phases have the same minimum value.

field part of the thermal contribution to the potential, making the stronger approximation Eq. (2.4), would be $V_T(h) = T^2 m_s^2/24 + T^2 \lambda h^2/48$ (plus a constant). The first term here is also a constant; the second looks like a correction (positive if $\lambda > 0$) to the h field mass squared. At temperatures where $T^2 \lambda/24 > -m_H^2$, there is a (meta)stable minimum at $h = 0$ and symmetry will be restored.

Often this mean-field approximation is insufficient. For instance, in this toy example it predicts that the phase transition should be of second order. Continuing to treat $m_a \ll \pi T$, but being more careful to account for the difference between $f_B(E)/E$ and $f_B(p)/p$, one finds a series expansion in $m_a/\pi T$:

$$V_T(h) = \sum_a \frac{T^2 m_a^2(h)}{24} - \frac{T m_a^3(h)}{12\pi} + \mathcal{O}(m^4/\pi^2) \quad (2.6)$$

which can predict a first-order phase transition, as illustrated in Figure 1. Since this transition is only first order because of changes in $f_B(E)/E$ (changes in the size of the fluctuations), it is called a fluctuation induced phase transition.

There are two potentially significant corrections to this simplistic description. One is that it has treated thermal particles as free, neglecting their mutual interactions. These give rise to higher order (“two loop”) corrections to the thermal potential computed here. These corrections can be important in establishing the order and strength of a phase transition when it is second or weakly first order. Second, there are subtleties in defining an effective potential if a scalar which may take on a vacuum value is a non-singlet under gauge interactions. Fortunately, for the electroweak transition to be phenomenologically interesting, it must be relatively strong. In this case neither of these subtleties is very important and

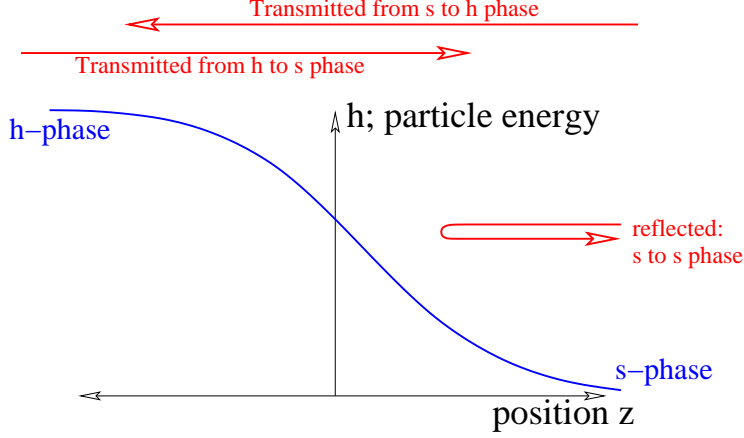


FIG. 2: Cartoon of a bubble wall: the scalar field h as a function of position $h(z)$. Particles “hit” the wall from either side, inducing net forces.

the one-loop treatment described here is generally adequate (unless the vacuum theory is strongly coupled, in which case we have little to say).

III. FRICTION ON A RELATIVISTIC BUBBLE WALL

When an effective potential has two local minima, there are two possible phases and there can be a phase interface between them, where the field varies from one to the other value, illustrated in Figure 2. Plasma particles approach the interface from either side. If the interface is not too sharp, particles follow classical trajectories in the wall background (wave packets are well described by the WKB approximation). In the interface rest frame, a particle’s energy and transverse momentum are conserved, so the classical trajectory is given by

$$\frac{d\vec{r}}{dt} = \frac{\mathbf{p}}{E}, \quad \frac{dE^2}{dt} = 0 \rightarrow \frac{2p_z dp_z}{dt} = -\frac{dm^2}{dt} = -\frac{dm^2}{dh} \frac{dh}{dz} \frac{dz}{dt}. \quad (3.1)$$

But $dz/dt = p_z/E$, so

$$\frac{dp_z}{dt} = -\frac{1}{2E} \frac{dm^2}{dh} \frac{dh}{dz}. \quad (3.2)$$

Note that dp_z/dt represents a net force on a plasma particle. The total force on all plasma particles, per unit surface area of the wall, is

$$\frac{F}{A} = - \int dz \frac{dh}{dz} \sum_a \frac{dm_a^2}{dh} \int \frac{d^3p}{(2\pi)^3 2E_a} f_a(\vec{p}, z) \quad (3.3)$$

with $f_a(\vec{p}, z)$ the occupancy of species a with momentum \vec{p} at distance z from the wall. a may be bosonic or fermionic and f_a is in general out of equilibrium. This is the force on particles due to the scalar background; there is an equal and opposite force on the background, which acts as a pressure difference restraining the motion of the interface. The wall also feels a force due to the vacuum potential; $F_{\text{vac}}/A = -\Delta V_{\text{vac}}$, pushing the wall forward. Therefore the total force pushing the phase interface forward is $(V_{\text{vac}}(h_1) - V_{\text{vac}}(h_2)) - F/A$.

In general the occupancies $f_a(\vec{p}, z)$ are all out of equilibrium and it is a nontrivial problem to determine them, simultaneously with the interface velocity, shape, and tension. This is what previous literature has attempted to do [23, 24, 25, 26, 27, 28, 29]. However, two limits are very simple.

The first simple limit is a bubble wall at rest in the plasma frame [26]. In this case, energy conservation, together with Liouville's theorem, imply that f_a remains always in equilibrium. Therefore Eq. (3.3) becomes

$$\frac{F}{A} = \int_{h_1}^{h_2} dh \sum_a \frac{dm_a^2}{dh} \int \frac{d^3p}{(2\pi)^3 2E_{p,h,a}} f_a(E_{p,h,a}), \quad (3.4)$$

with f_a the equilibrium distribution function. This expression coincides with the expression we found earlier for the thermal potential difference between phases $V_T(h_2) - V_T(h_1)$, so the total force on the wall is $V(h_1) - V(h_2)$. The critical temperature T_c is defined as the temperature where the potential is equal in the two minima. Therefore, at T_c the forces are in balance and a wall at rest will remain at rest, as expected.

The other simple limit is the limit we need in this paper; a wall with velocity v which is ultra-relativistic in the plasma frame, *i.e.*, with gamma factor $\gamma \gg 1$. In practice we will be interested in really macroscopic values $\gamma \sim 10^9$, so in the following we make no qualms about strictly expanding to lowest nontrivial order in γ . We begin by analyzing what happens in the rest-frame of the bubble wall. In this frame the plasma is ultra-relativistic with velocity v , which we take to point along the $-z$ direction (so the plasma-frame wall has positive v_z velocity). The mean wall-frame particle energy is $E \sim \gamma T$, which will always be enough⁵ to allow the particle to pass over the wall, $\gamma T \gg m_a(h_2)$. Furthermore, the mean momentum $p_z \sim \gamma T$ is so large that the WKB approximation is excellent and the reflection coefficients are exponentially suppressed. Interactions or scatterings between plasma particles occur at a time-dilated rate $t \sim 1/\gamma T$ (times inverse powers of couplings) and can be neglected. Therefore the occupancies evolve undisturbed. Also, the number of particles approaching the wall from the positive z side is exponentially suppressed by $\exp(-\gamma m_a/T)$. That means that the particles approaching the wall have received no signal that the wall is approaching, and are in equilibrium.

Rather than integrate the pressure per length over the wall, we can directly compute the net pressure on the wall by summing up the momentum change of each particle which passes over the wall [26]:

$$-\frac{F}{A} = \sum_a \int \frac{d^3p}{(2\pi)^3} f_a(p, \text{in}) (p_{z,\text{in}} - p_{z,\text{out}}). \quad (3.5)$$

Here p , $f_a(p, \text{in})$ are the *incoming* momentum and occupancy.⁶ Eq. (3.5) is what we would get by performing the z -integration in Eq. (3.3), keeping f_a constant along a classical trajectory

⁵ In general no excitation should be treated as perfectly massless. Therefore, for $\gamma \gg T/m$, the statements here have only exponentially small corrections, $\sim \exp(-\gamma m/T)$, as opposed to the power (phase space) suppressed corrections one would expect if $m = 0$ strictly.

⁶ The integration includes backwards-pointing $p_z < 0$ but they will have exponentially small $f(p)$ and so the error from their inclusion is negligible; the same applies for p_z which are positive but so small that the particle would reflect.

and taking advantage of the absence of reflections.

Since the wall is at rest and uniform in the transverse directions, both energy and p_\perp are conserved. Together with $\gamma \gg 1$, this makes evaluating $(p_{z,\text{in}} - p_{z,\text{out}})$ simple:

$$\begin{aligned} p_{z,\text{in}}^2 + m^2(h_1) &= p_{z,\text{out}}^2 + m^2(h_2), \\ p_{z,\text{in}} + \frac{m^2(h_1)}{2p_{z,\text{in}}} + \mathcal{O}(m^4/p^3) &= p_{z,\text{out}} + \frac{m^2(h_2)}{2p_{z,\text{out}}} + \mathcal{O}(m^4/p^3), \\ p_{z,\text{in}} - p_{z,\text{out}} &= -\frac{m^2(h_2) - m^2(h_1)}{2E} + \mathcal{O}(m^2/E^3, p_\perp^2/E^3), \end{aligned} \quad (3.6)$$

where in the last line we have used $E^{-1} = -p_z^{-1} + \mathcal{O}(m^2/E^3, p_\perp^2/E^3)$. The terms $\sim E^{-3}$ will be γ^{-2} suppressed and can be dropped. Therefore the pressure difference is

$$\frac{F}{A} = \sum_a (m_a^2(h_2) - m_a^2(h_1)) \int \frac{d^3p}{(2\pi)^3 2E_{p,h_1,a}} f_a(p, \text{in}) + \mathcal{O}(1/\gamma^2). \quad (3.7)$$

The integration measure and occupancies are covariant⁷ and can be performed in any frame; it is most convenient to do so back in the plasma frame. This shows that Eq. (3.7) is identical to Eq. (2.5).

Therefore the backwards pressure on the interface in the limit $\gamma \gg 1$ is found by replacing the thermal effective potential $V = V_{\text{vac}} + V_T$ with $\tilde{V} = V_{\text{vac}} + V_T[\text{mean field}]$. This is the main result of this section.⁸

Let us comment quickly on scaling. The density of particles increases as γ , due to Lorentz contraction. But the mean momentum that each particle induces, in climbing the wall, goes as $1/\gamma$ (since $\delta p_z \sim m^2/E \sim 1/\gamma$), which explains why there is a finite large- γ limit.

As a check, we can repeat the calculation in the plasma frame. Since the wall passes at the speed of light and purely in the $+z$ direction, it leaves each particle's p_\perp and $E - p_z$ unchanged.⁹ However $E^2 - p^2$ must change by Δm^2 , which uniquely determines the changes to a particle's 4-momentum:

$$(E, p_z, p_\perp) \rightarrow \left(E + \frac{m^2(h_2) - m^2(h_1)}{2(E - p_z)}, p_z + \frac{m^2(h_2) - m^2(h_1)}{2(E - p_z)}, p_\perp \right). \quad (3.8)$$

In computing the momentum transfer to the phase interface, we must remember to consider the flux of particles through the wall, not the particle density. The flux differs from the

⁷ Note that $p, f(p)$ are defined based on their symmetric phase ($z > 0$) values. The expression is covariant only if we identify $E = E_{p,h_1,a}$ since that is the energy which satisfies the mass shell condition in the symmetric phase, where p is defined.

⁸ Some readers might worry that this leading-order analysis may receive large higher-loop effects of form $\alpha \ln \gamma$. In particular, since the wall “sees” particles with extremely high energies, shouldn't it analyze their partonic content? We believe that the answer is “no.” Partonic content becomes important when a particle is analyzed not with a large energy, but with a large available transverse momentum needed to put the partonic contents on-shell. The wall is uniform in the transverse direction and so cannot impart any transverse momentum; so the actual transverse analysis scale is infrared and partonic content is not probed.

⁹ $E - p_z$ conservation is the same as energy conservation in the wall rest frame.

particle density by a factor of $v_{\text{relative}} = 1 - v_z = 1 - p_z/E$. Therefore the force per unit area is

$$\begin{aligned} \frac{F}{A} &= \sum_a \int \frac{d^3p}{(2\pi)^3} f_a(E_{\text{in}}) v_{\text{relative}} \frac{m_a^2(h_2) - m_a^2(h_1)}{2(E - p_z)} \\ &= \sum_a \left(m_a^2(h_2) - m_a^2(h_1) \right) \int \frac{d^3p}{(2\pi)^3} f_a(E_{\text{in}}) \frac{E - p_z}{E} \frac{1}{2(E - p_z)} \end{aligned} \quad (3.9)$$

which is the same as Eq. (3.7).

IV. EXAMPLE: SINGLET EXTENSION OF THE STANDARD MODEL

Here we apply the above results to the simplest extension of the Standard Model which can provide a strong electroweak phase transition; the model extended by one real singlet scalar field s . This field need not have an $s \leftrightarrow -s$ discrete symmetry. If not, then s^3 and $sH^\dagger H$ potential terms can appear at tree level, potentially leading to a strongly first order electroweak phase transition, as recently studied in [32].¹⁰

So consider the scalar sector of an extension to the Standard Model; besides the complex doublet Higgs field H there is a real singlet field s , with tree-level potential

$$V = V_H + V_{HS} + V_S \quad (4.1)$$

with

$$V_H = -\mu_h^2 H^\dagger H + \lambda_h (H^\dagger H)^2 \quad (4.2)$$

$$V_{HS} = \frac{a}{2} H^\dagger H s + \frac{\lambda}{2} H^\dagger H s^2 \quad (4.3)$$

$$V_S = \frac{-\mu_s^2}{2} s^2 + \frac{b}{3} s^3 + \frac{\lambda_s}{4} s^4. \quad (4.4)$$

We want to probe whether or not the bubble wall runs away in this model as a function of the parameters $\lambda, \lambda_h, \lambda_s, \mu_s^2, \mu_h^2, a, b$, and in particular we want to see how the wall velocity is correlated with the strength of the transition (and possibly other attributes).

To do so we perform a Monte-Carlo sampling over the values of the 7 scalar Lagrangian parameters, fixing μ_h^2/λ_h to give the right physical Higgs VEV. For each choice of scalar parameters, we take a series of steps:

1. First we must make sure that the parameters give a vacuum consistent with phenomenology. We enforce absolute stability of the theory, requiring $\lambda_h > 0$, $\lambda_s > 0$, and $\lambda > -\sqrt{4\lambda_h\lambda_s}$. Then we require that the Higgs vacuum is deeper than any s -only vacua and that the scalar states in the Higgs minimum obey experimental Higgs mass constraints [34]¹¹.

¹⁰ Actually the transition can be strong even without these cubic terms; furthermore, in the theory with $s \leftrightarrow -s$ discrete symmetry, the s particles are an interesting dark matter candidate [33].

¹¹ We impose a simplified version of the limits found in [34]. First one computes the masses of the two scalar states and their mixing angles with the pure Higgs direction. Then we approximate the constraint found in [34] to require $\cos^2 \theta < 0.25$ if $m < 115\text{GeV}$ and $\cos^2 \theta < 0.04$ if $m < 90\text{GeV}$.

2. We compute the thermal effective potential and place the following constraints on the minimum structure as a function of temperature. The h minimum (by which we mean any minimum with a nonzero condensate of the Higgs field) must become unstable (become an inflection point rather than a minimum) at some point as the temperature is raised; we call this temperature where it suffers spinodal instability T_{spin1} . Then we require that the s -minimum which is stable above T_{spin1} should become spinodally unstable as the temperature is lowered, at some $T_{\text{spin2}} > 0$. The latter condition ensures that the universe does not become trapped in an electroweak-symmetric phase as it cools. (The criterion is a little too strong; we really only need ensure that the nucleation action to leave the s -phase for the h -phase is small enough at some temperature to allow the transition to occur. Spinodal instability means the nucleation rate diverges, so it is a sufficient condition for this to occur.)

We are mostly interested in the behavior around the transition temperature and in cases which are marginal between runaway and finite-velocity bubble walls. Therefore we expect moderate scalar VEVs $h/T \sim 1$, which allows the use of the high temperature expansion for the thermal potential, which we take to be [2, 35]

$$V_T = h^2 T^2 \left(\frac{9g^2 + 3g'^2 + 12y_{\text{top}}^2 + 24\lambda_h + 2\lambda}{96} \right) + s^2 T^2 \left(\frac{2\lambda + 3\lambda_s}{24} \right) + \frac{(a+b)sT^2}{12} - \frac{h^3 T}{12\pi} \left(\frac{3}{4}g^3 + \frac{3}{8}(g^2 + g'^2)^{3/2} \right). \quad (4.5)$$

Here g, g', y_{top} are the weak, hypercharge, and top quark Yukawa couplings respectively; all other terms arise from integrating out the scalars. Note that this potential makes a few approximations, dropping the effects of Debye screening and the cubic terms for scalar fields. It is not our intention to perform a state of the art analysis, and the dropped effects are not too important if the transition is relatively strong with relatively light scalar masses near T_c , which is the case when the bubble wall is marginal between finite velocity and runaway with a transition strong enough to be physically interesting ($h/T > 1$).

Since very weak transitions are physically uninteresting, we discard all transitions with $h(T_{\text{spin1}})/T_{\text{spin1}} < 0.2$ from further analysis.

3. We determine the critical temperature, where the s and h phases have equal free energy. Then we find the nucleation temperature T_{nuc} , which we take to be the temperature where the energy of a critical bubble is $S_{\text{nuc}} = E/T = 100$.¹² The definition of the critical bubble energy is standard [31] and we use the algorithm for multi-field bubble finding presented Appendix 2 of [36].

¹² It is often stated that bubble nucleation occurs when $\exp(-S_{\text{nuc}}) = (T/H)^4$ so there is one bubble nucleation per Hubble volume per Hubble time. This is wrong; one should define $\Gamma_{\text{nuc}} = -dS_{\text{nuc}}/dt = HTdS_{\text{nuc}}/dT$, which is the time it takes for the nucleation rate to change appreciably; then one demands that $\exp(-S_{\text{nuc}}) = (T/\Gamma)^4$ so there are enough bubbles to fill the universe in the time it takes for the nucleation rate to change appreciably. This guided our choice of 100 (see also [27]).

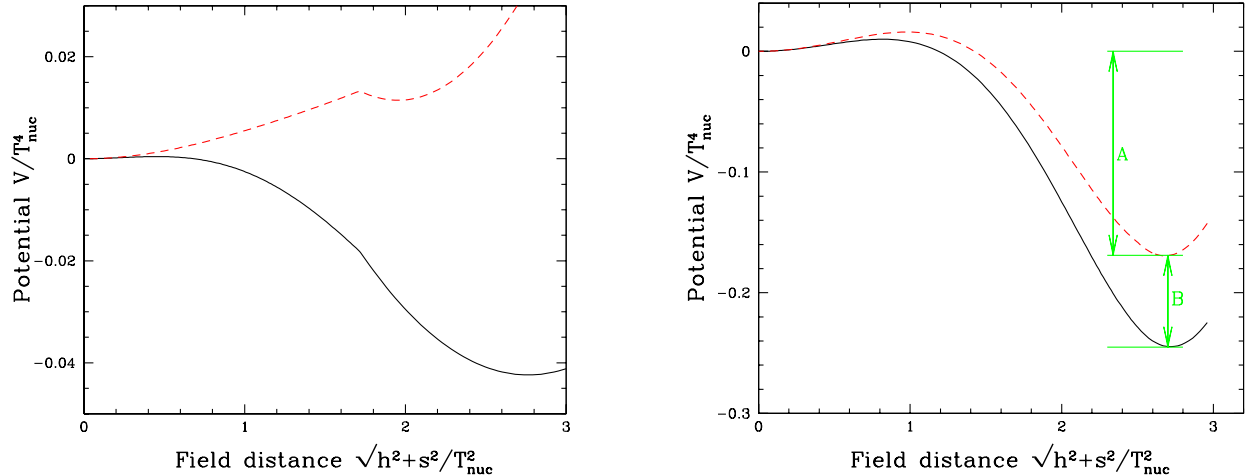


FIG. 3: Example of the effective potential V and pseudo-potential \tilde{V} used to determine bubble wall runaway, for two sets of parameters which produce the same value of h/T_{nuc} . The left plot is a case where the bubble wall remains of finite velocity; in the right case it runs away. Note the different scales on the vertical axis; the scalar excitations in the two minima are much lighter for the left case than for the right.

- Using the potential at T_{nuc} and the procedure of the last section, we determine whether or not the bubble wall can run away. In detail, we must determine two “potentials” at T_{nuc} ; the actual potential $V(T_{\text{nuc}}) = V_{\text{vac}} + V_T(T_{\text{nuc}})$ and the mean-field potential expanded about the s minimum using Eq. (4.5), \tilde{V} . For our case and thanks to our neglect of cubic terms arising from the scalar fields, $\tilde{V}(h, s)$ is the same as Eq. (4.5) without the $h^3 T/12\pi$ type terms.

We plot both the true and mean-field potential for two illustrative cases in Fig. 3. The black curves are the actual thermal (equilibrium) effective potentials, evaluated along the curve in the h, s plane taken by the critical bubble profile.¹³ Naturally, in both cases they indicate that the h -phase is deeper (preferred). The red curves are the mean-field potentials \tilde{V} defined in the last section, which we can think of as *non-equilibrium* effective potentials. The value of the red curve at a given value of h, s is the free energy cost per unit volume to force a phase interface to sweep through the plasma, if the phase interface changes the plasma from the $h = 0$ phase to a phase with the given h, s value. For values of (h, s) where it is positive, it would cost energy to create a phase with these VEVs if the phase is to be produced by an ultra-relativistic interface. Where the potential is negative, there is leftover free energy available from creating the h -phase, which goes into accelerating the bubble wall. Therefore the left figure represents a case where the bubble wall cannot run away. The right figure represents a case where it will run away. Note however that the value of h where the red curve is minimized is not the same as the equilibrium h VEV. This means that,

¹³ V is evaluated along the path through the (h, s) plane which is actually explored by the critical bubble; the x -axis is the affine distance in the (h, s) plane along this curve. The cusp in the left figure is at the (h, s) value at the center of the critical bubble; we used a straight-line extension from there to the minimum of the potential, so the path in the (h, s) plane had a cusp at this point.

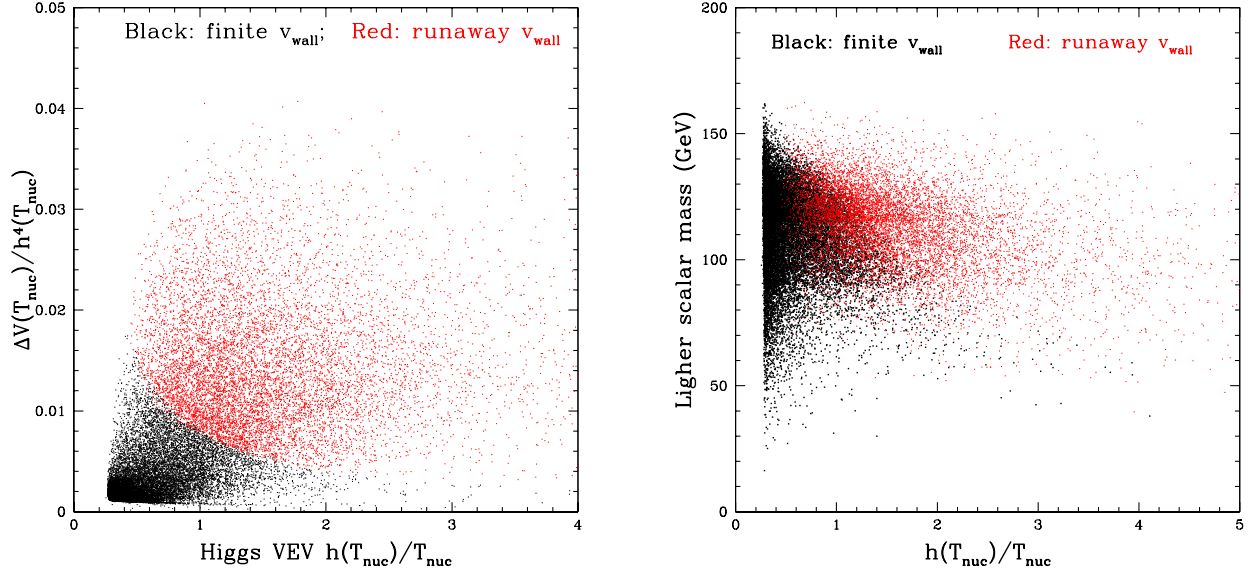


FIG. 4: Scatter-plots of h/T versus the free energy available in the transition (left) and versus the lighter physical vacuum scalar mass (right). In both figures, red dots are parameter values which give runaway bubble wall velocities, while black values give finite bubble wall velocities. For the transition to provide a large free energy or to arise from relatively heavy scalars, the bubble wall must generally be of the runaway type.

immediately behind the bubble wall, the value of h would be slightly lower than in equilibrium. The VEV h will relax to the equilibrium value as the non-equilibrium state after the bubble wall passage re-equilibrates. The height indicated as A in the diagram is free energy density available to accelerating the phase interface; the height indicated as B is free energy density lost to entropy production in re-equilibrating the system after the wall's passage.

Some results from our Monte-Carlo study of the parameter space of this toy model are shown in Figure 4. The study shows, as expected, that weak transitions generally involve finite wall velocities, while strong transitions almost always require runaway bubble wall velocities. However a small subset of strong transitions (as measured by h/T , the relevant quantity for baryogenesis since it determines whether baryon number is violated after the transition [37]) have finite bubble wall velocities rather than runaways. These strong but non-runaway transitions occur when the potential between the two (s and h) minima is very flat. The figure also shows that, in these cases, there is also generally a light physical scalar state in vacuum, which must be nearly aligned with the s direction in order to meet Higgs search bounds. (The cutoff in h/T at small values is imposed by our procedure since we discard very weak transitions.)

V. CONCLUSIONS

The physical consequences of the electroweak phase transition depend on the propagation speed of the phase interface. Theories with singlet scalars can have very strong transitions

without requiring large couplings or violating the Higgs mass bound, because the potential can already possess multiple metastable minima at the mean-field level. We show here that such strong mean-field type transitions generally – but not always – involve interfaces which propagate at virtually the speed of light, as occurs in vacuum transitions. However, in the MSSM or other theories where the first order nature of the transition is fluctuation induced, the bubble wall can never run away. We provide a clean, simple criterion, valid at the 1-loop level of analysis, which determines whether or not bubble walls run away. Specifically, one defines \tilde{V} , the vacuum effective potential V_{vac} plus the quadratic-order Taylor expansion of the thermal part V_T of the potential about the high-temperature phase. If the low-temperature phase is preferred at T_{nuc} by \tilde{V} , then the wall runs away; otherwise it has a finite terminal velocity. For the case of a real singlet extension of the Standard Model, we find that very strong phase transitions (say, $h/T > 2$) either have runaway bubble walls or have very slight supercooling, a small available free energy at the transition, and very light physical scalar excitations.

It would be interesting to apply this work to the nMSSM. For cases where couplings are relatively large or where two-loop thermal effects are important, it would also be necessary to understand how to incorporate these effects in to our treatment.

Acknowledgments

We are indebted to Geraldine Servant, Neil Barnaby and Lev Kofmann for stimulating us to think about this issue after so many years, and to Neil Turok, for useful conversations (which occurred about 14 years ago). GM would like to thank the Faculty of Physics at Bielefeld University for hospitality, and the Alexander von Humboldt Foundation for its support through a F. B. Bessel prize. This work was supported in part by the Natural Sciences and Engineering Research Council of Canada.

APPENDIX A: THERMODYNAMICS OF RUNAWAY WALLS

This Appendix explores the thermodynamics which establishes whether runaway bubble walls are thermodynamically consistent. Consider two phases, with pressures $P_1(T)$ and $P_2(T)$; the entropy density $s = dP/dT$ and energy density $\epsilon = sT - P$ follow from $P(T)$. Here $P_1(T)$ is for the high temperature s -phase, $P_2(T)$ for the low-temperature h -phase, so for $T < T_c$ we have $P_2(T) > P_1(T)$. The phases are separated by a planar interface moving in the $+z$ direction at the speed of light, with surface energy density $\sigma(t)$. We work in the rest frame of the unburnt s -phase plasma; the h -phase plasma fills the region $z < t$ and flows with forward velocity v_2 . The temperature of the unburnt plasma is T_1 , the burnt plasma is T_2 . We want to determine for what values of T_1 the interface gains surface energy density, $d\sigma/dt > 0$.

This problem has three unknowns; T_2 , v_2 , and $d\sigma/dt$. We have two equations and one inequality with which to determine them; conservation of energy and of z -momentum, and the positivity of entropy production. The equation of state provides the stress tensor in each phase:

$$\begin{aligned} T_i^{\mu\nu} &= (\epsilon_i + P_i)u_i^\mu u_i^\nu + P_i g^{\mu\nu}, & u_1 &= (1, 0, 0, 0), & u_2 &= (\gamma_2, 0, 0, \gamma_2 v_2), \\ \epsilon_i &= \epsilon_i(T_i), & P_i &= P_i(T_i). \end{aligned} \tag{A1}$$

The index i indicates which phase's equation of state is to be used. Per unit time, the energy per area of phase 2 increases by T_2^{00} , while the energy per area of phase 1 decreases by T_1^{00} . These must be balanced by the momentum flows and the energy change of the bubble wall:

$$\begin{aligned}\frac{d\sigma}{dt} &= T_1^{00} - T_2^{00} + T_2^{0z} - T_1^{0z} \\ &= \epsilon_1 - (\gamma_2^2 - \gamma_2^2 v_2) \epsilon_2 + (1 - \gamma_2^2 + \gamma_2^2 v_2) P_2.\end{aligned}\tag{A2}$$

Similarly the z -momentum must be balanced:

$$\begin{aligned}\frac{d\sigma}{dt} &= T_1^{z0} - T_2^{z0} + T_2^{zz} - T_1^{zz} \\ &= -P_1 + (\gamma_2^2 v_2^2 - \gamma_2^2 v_2) \epsilon_2 + (1 + \gamma_2^2 v_2^2 - \gamma_2^2 v_2) P_2.\end{aligned}\tag{A3}$$

Adding these yields a simpler expression:

$$2\frac{d\sigma}{dt} = \epsilon_1 - P_1 - \epsilon_2 + P_2.\tag{A4}$$

The total entropy of the system must also increase. The entropy density of phase 2 is $\gamma_2(\epsilon_2 + P_2)/T_2$ (the factor γ_2 because of Lorentz contraction) and the volume increase of phase 2 per unit time is $(1 - v_2)$. Therefore entropy increase requires

$$\gamma_2(1 - v_2) \frac{\epsilon_2(T_2) + P_2(T_2)}{T_2} > \frac{\epsilon_1(T_1) + P_1(T_1)}{T_1}\tag{A5}$$

where the RHS is the reduction of entropy stored by the shrinking s -phase.

The bubble wall runaway is permitted if there is a solution with $d\sigma/dt > 0$, so energy accumulates in the bubble wall rather than being lost. Unfortunately two equations and an inequality are not enough to solve for the three unknowns $d\sigma/dt$, v_2 , and T_2 . If we somehow knew how much entropy is generated at the wall, we could replace Eq. (A5) with an equation and all variables would be determined. This requires some microscopic dynamics details, which are treated in the main text of the paper. Here we will just determine under what conditions a runaway wall is thermodynamically consistent. That is, we can determine the domain of T_1 values where it is at least thermodynamically consistent for a bubble wall to run away. We do this by setting the entropy production to zero, which determines the bubble wall velocity: treated as an equality, Eq. (A5) becomes

$$v_2 = \frac{1 - x^2}{1 + x^2}, \quad x \equiv \frac{(\epsilon_1 + P_1)T_2}{(\epsilon_2 + P_2)T_1} = \frac{s_1}{s_2}.\tag{A6}$$

Then the remaining two equations determine $d\sigma/dt$ in terms of the initial temperature T_1 .

Specifically, since the h -phase becomes more favorable as the temperature drops, we can search for the temperature at which ultra-relativistic bubble propagation first becomes thermodynamically feasible, which is where $d\sigma/dt = 0$ at zero entropy generation. Then T_2 is determined from T_1 by using Eq. (A4): $\epsilon_2(T_2) - P_2(T_2) = \epsilon_1(T_1) - P_1(T_1)$. The critical value of T_1 is the value where the so-determined T_2 , v_2 will give a valid solution to Eq. (A2).

We evaluated this value T_1 for each set of parameter values in the toy model discussed in Sec. IV. We also determined T_{reheat} , determined by the criterion

$$\epsilon_1(T_{\text{reheat}}) = \epsilon_2(T_c).\tag{A7}$$

That is, T_{reheat} is the temperature where the supercooled s -phase has the same energy density as the h -phase at T_c . Its physical importance is that, for slow bubble walls, if $T_{\text{nuc}} > T_{\text{reheat}}$ then the universe will heat back up to T_c before the phase transition completes and there will be a period of mixed phase; whereas if $T_{\text{nuc}} < T_{\text{reheat}}$ then the supercooling is enough to use up all of the latent heat of the transition without reheating to T_c and no quasi-equilibrium mixed-phase situation occurs.

Surprisingly, we find in the toy model that in every case $T_c > T_1 > T_{\text{reheat}}$. That is, the criterion that ultra-relativistic bubble walls are thermodynamically consistent is in practice a *weaker* condition than the condition of sufficient supercooling not to reheat to T_c . Further, we find $T_{\text{reheat}} > T_{\text{nuc}}$ for all but a very small corner of the parameter space of the theory. Therefore, in the singlet-scalar model, supercooling proceeded below either temperature throughout almost the entire parameter space which provides a first order phase transition. The fact that many parameters give bubble walls which cannot run away means that the production of entropy at the bubble wall significantly reduces the range in which walls run away, relative to what is thermodynamically consistent.

-
- [1] D. A. Kirzhnits and A. D. Linde, Phys. Lett. B **42**, 471 (1972).
 - [2] L. Dolan and R. Jackiw, Phys. Rev. D **9**, 3320 (1974).
 - [3] S. Weinberg, Phys. Rev. D **9**, 3357 (1974).
 - [4] T. Banks and E. Rabinovici, Nucl. Phys. B **160**, 349 (1979); E. H. Fradkin and S. H. Shenker, Phys. Rev. D **19**, 3682 (1979).
 - [5] K. Kajantie, M. Laine, K. Rummukainen and M. E. Shaposhnikov, Phys. Rev. Lett. **77**, 2887 (1996) [arXiv:hep-ph/9605288].
 - [6] V. A. Kuzmin, V. A. Rubakov and M. E. Shaposhnikov, *On The Anomalous Electroweak Baryon Number Nonconservation In The Early Universe*, Phys. Lett. B **155** (1985) 36.
 - [7] For reviews see for instance, A. G. Cohen, D. B. Kaplan and A. E. Nelson, Ann. Rev. Nucl. Part. Sci. **43**, 27 (1993) [arXiv:hep-ph/9302210]; V. A. Rubakov and M. E. Shaposhnikov, Usp. Fiz. Nauk **166**, 493 (1996) [Phys. Usp. **39**, 461 (1996)] [arXiv:hep-ph/9603208].
 - [8] M. S. Turner and L. M. Widrow, Phys. Rev. D **37**, 2743 (1988).
 - [9] G. Baym, D. Bodeker and L. D. McLerran, Phys. Rev. D **53**, 662 (1996) [arXiv:hep-ph/9507429].
 - [10] C. J. Hogan, Mon. Not. Roy. Astron. Soc. **218**, 629 (1986).
 - [11] A. Kosowsky, M. S. Turner and R. Watkins, Phys. Rev. Lett. **69**, 2026 (1992); M. Kamionkowski, A. Kosowsky and M. S. Turner, Phys. Rev. D **49**, 2837 (1994) [arXiv:astro-ph/9310044].
 - [12] C. Grojean and G. Servant, Phys. Rev. D **75**, 043507 (2007) [arXiv:hep-ph/0607107]; S. J. Huber and T. Konstandin, JCAP **0805**, 017 (2008) [arXiv:0709.2091 [hep-ph]]; C. Caprini, R. Durrer and G. Servant, Phys. Rev. D **77**, 124015 (2008) [arXiv:0711.2593 [astro-ph]]; T. Kahniashvili, A. Kosowsky, G. Gogoberidze and Y. Maravin, Phys. Rev. D **78**, 043003 (2008) [arXiv:0806.0293 [astro-ph]].
 - [13] K. Farakos, K. Kajantie, K. Rummukainen and M. E. Shaposhnikov, Nucl. Phys. B **425**, 67 (1994) [arXiv:hep-ph/9404201]; K. Kajantie, M. Laine, K. Rummukainen and M. E. Shaposhnikov, Nucl. Phys. B **458**, 90 (1996) [arXiv:hep-ph/9508379]; Nucl. Phys. B **466**, 189 (1996)

- [arXiv:hep-lat/9510020].
- [14] A. G. Cohen, D. B. Kaplan and A. E. Nelson, Phys. Lett. B **245**, 561 (1990); A. E. Nelson, D. B. Kaplan and A. G. Cohen, Nucl. Phys. B **373**, 453 (1992).
- [15] M. Joyce, T. Prokopec and N. Turok, Phys. Rev. D **53**, 2930 (1996) [arXiv:hep-ph/9410281]; Phys. Rev. D **53**, 2958 (1996) [arXiv:hep-ph/9410282].
- [16] M. S. Carena, J. M. Moreno, M. Quiros, M. Seco and C. E. M. Wagner, Nucl. Phys. B **599**, 158 (2001) [arXiv:hep-ph/0011055].
- [17] S. J. Huber and M. G. Schmidt, Nucl. Phys. B **606**, 183 (2001) [arXiv:hep-ph/0003122].
- [18] J. M. Cline and K. Kainulainen, Phys. Rev. Lett. **85**, 5519 (2000) [arXiv:hep-ph/0002272]; J. M. Cline, M. Joyce and K. Kainulainen, JHEP **0007**, 018 (2000) [arXiv:hep-ph/0006119].
- [19] M. Gyulassy, K. Kajantie, H. Kurki-Suonio and L. D. McLerran, Nucl. Phys. B **237** (1984) 477; J. Ignatius, K. Kajantie, H. Kurki-Suonio and M. Laine, Phys. Rev. D **49**, 3854 (1994) [arXiv:astro-ph/9309059]; H. Kurki-Suonio and M. Laine, Phys. Rev. D **51**, 5431 (1995) [arXiv:hep-ph/9501216]; H. Kurki-Suonio and M. Laine, Phys. Rev. Lett. **77**, 3951 (1996) [arXiv:hep-ph/9607382].
- [20] P. J. Steinhardt, “Relativistic Detonation Waves And Bubble Growth In False Vacuum Decay,” Phys. Rev. D **25** (1982) 2074.
- [21] M. Laine, Phys. Rev. D **49**, 3847 (1994) [arXiv:hep-ph/9309242].
- [22] S. R. Coleman, “The Fate Of The False Vacuum. 1. Semiclassical Theory,” Phys. Rev. D **15** (1977) 2929 [Erratum-ibid. D **16** (1977) 1248].
- [23] B. H. Liu, L. D. McLerran and N. Turok, Phys. Rev. D **46**, 2668 (1992).
- [24] M. Dine, R. G. Leigh, P. Y. Huet, A. D. Linde and D. A. Linde, Phys. Rev. D **46**, 550 (1992) [arXiv:hep-ph/9203203].
- [25] S. Y. Khlebnikov, Phys. Rev. D **46**, 3223 (1992).
- [26] P. Arnold, Phys. Rev. D **48**, 1539 (1993) [arXiv:hep-ph/9302258].
- [27] G. D. Moore and T. Prokopec, Phys. Rev. D **52**, 7182 (1995) [arXiv:hep-ph/9506475].
- [28] P. John and M. G. Schmidt, Nucl. Phys. B **598**, 291 (2001) [Erratum-ibid. B **648**, 449 (2003)] [arXiv:hep-ph/0002050].
- [29] G. D. Moore, JHEP **0003**, 006 (2000) [arXiv:hep-ph/0001274].
- [30] S. J. Huber and M. G. Schmidt, Nucl. Phys. B **606**, 183 (2001) [arXiv:hep-ph/0003122].
- [31] I. Affleck, Phys. Rev. Lett. **46**, 388 (1981); A. D. Linde, Nucl. Phys. B **216**, 421 (1983) [Erratum-ibid. B **223**, 544 (1983)].
- [32] S. Profumo, M. J. Ramsey-Musolf and G. Shaughnessy, JHEP **0708**, 010 (2007) [arXiv:0705.2425 [hep-ph]].
- [33] V. Silveira and A. Zee, Phys. Lett. B **161**, 136 (1985); J. McDonald, Phys. Rev. D **50**, 3637 (1994) [arXiv:hep-ph/0702143]; C. P. Burgess, M. Pospelov and T. ter Veldhuis, Nucl. Phys. B **619**, 709 (2001) [arXiv:hep-ph/0011335].
- [34] R. Barate *et al.* [LEP Working Group for Higgs boson searches], Phys. Lett. B **565**, 61 (2003) [arXiv:hep-ex/0306033].
- [35] D. A. Kirzhnits and A. D. Linde, Annals Phys. **101**, 195 (1976).
- [36] J. M. Cline, G. D. Moore and G. Servant, Phys. Rev. D **60**, 105035 (1999) [arXiv:hep-ph/9902220].
- [37] M. E. Shaposhnikov, Nucl. Phys. B **287**, 757 (1987).